

Random magnetic order in Al-Mn liquids

A. V. Smirnov*

Institut für Festkörperphysik, Technische Hochschule, D-64289 Darmstadt, Germany

A. M. Bratkovsky†

Oxford University, Department of Materials, Oxford OX1 3PH, England

(Received 25 October 1995)

We have performed *ab initio* calculations of a possible complex noncollinear magnetic structure in aluminium-rich Al-Mn liquids within the real-space tight-binding linear muffin-tin orbital method. In our previous work we predicted the existence of large magnetic moments in Al-Mn liquids [A. M. Bratkovsky, A. V. Smirnov, D. N. Manh, and A. Pasturel, Phys. Rev. B **52**, 3056 (1995)], which has been very recently confirmed experimentally. Our present calculations show that there is a strong tendency for the moments on Mn to have a noncollinear (random) order retaining their large value of about $3\mu_B$. The *d* electrons on Mn demonstrate a pronounced non-rigid-band behavior which cannot be reproduced within a simple Stoner picture. The origin of the magnetism in these systems is a topological disorder which drives the moments formation and frustrates their directions in the liquid phase.

I. INTRODUCTION

The behavior of magnetic atoms dissolved in simple metals has been a subject of experimental and theoretical studies for many decades. The relevant phenomena raise the question of how the magnetic state of the impurity or lattice of the magnetic atoms depends on the host metal and atomic configuration. The basic understanding of the phenomenon came with Friedel's concept of a virtual bound state¹ and the Anderson impurity model,² which allowed the classification of the different possibilities to some extent.

There are, however, a few important open questions and one of those is about the effect of disorder, especially *topological disorder*, on the magnetic state of the system. A conspicuous example is Mn in an Al matrix. Friedel estimated that Mn in Al is nonmagnetic¹ but as a result of later studies this view was revised. Cooper and Miljak found that a Mn impurity in fcc Al carries a big moment of $\mu = 3.2 \pm 0.2$ and the moment on Mn gets apparently screened by *sp* electrons up to very high temperatures, suggesting surprisingly high values of the Kondo temperature, $T_K = 600$ K.³

With the discovery of Al-Mn quasicrystals⁴ the problem of the magnetic behavior of Mn in Al became rather acute and is a focus of extensive research. Hauser *et al.*⁵ studied the Mn magnetic moment in crystalline (*c*), icosahedral (*i*), and amorphous (*a*) phases of $\text{Al}_{100-x}\text{Mn}_x$ alloys. They revealed that Mn in the disordered phases has a well defined local magnetic moment ($\mu_{\text{eff}}/\mu_B \sim 0.7, 1.1, 2.4$ at $x = 16, 20, 45$) with no moment in crystalline Al_6Mn and a fairly large magnetic moment of $1.55\mu_B$ for crystalline $\text{Al}_{95}\text{Mn}_5$. Hauser *et al.* have speculated that the interaction of Mn atoms in Al-Mn is the reason for the appearance of magnetic Mn sites. Some data suggest the existence of a Mn magnetic moment in liquid Al-Mn of about $\mu_{\text{eff}}/\mu_B \sim 2.9, 3.2$ for $x = 20$ and 40 ,⁶ respectively. Many authors have reported that, for the *i* and *a* phases, only a small fraction of the Mn atoms are really magnetic at low temperatures and that they

have a large moment ranging from $2.5\mu_B$ (Ref. 7) to even $7\mu_B$.⁸

On the theoretical side there are contradictory results for the magnetic behavior of Mn in an Al matrix. In Refs. 9–12 the moment on Mn in fcc Al was found with values varying in the interval $1.74\text{--}3.26\mu_B$, whereas in the calculations¹³ and in Ref. 14 Mn was found to be paramagnetic. Liu *et al.*¹⁴ found no moment on Mn in MnAl_n clusters with $n < 54$, however, in clusters containing more than one manganese atom the moment appeared. On the other hand, the results of Ref. 15 support the idea of a virtual bound-state model¹⁰ as an explanation of Mn magnetism in the single-impurity limit.

Recently, we have performed *ab initio* calculations for liquid $\text{Al}_{100-x}\text{Mn}_x$ ($x = 14, 20, \text{ and } 40$) to gain more insight into the problem of Mn magnetism in a disordered Al host.¹⁶ Our real-space (RS) spin-polarized calculations showed unambiguously the formation of a large moment of about $3\mu_B$ on Mn in these Al-Mn liquids. We showed that the reason for the moment formation lies in a smearing out of the van Hove dip in the density of states which kills the moment in *c*- Al_6Mn . It means that *topological disorder* is the origin of the moment formation on Mn in an Al matrix.

This prediction has been very recently confirmed experimentally by Hippert *et al.*¹⁷ who investigated the series of alloys $\text{Al}_{1-x-y}\text{Pd}_x\text{Mn}_y$ and found that a localized moment appears on Mn atoms in the liquid state and disappears in the solid state. The moment they have found is $2.76 \pm 0.01\mu_B$ from susceptibility measurements and 2.74 ± 0.1 from the neutron-scattering data, in agreement with our predictions.¹⁶ The authors¹⁷ have also observed that, first, the moment is *independent* of the Mn concentration thus demonstrating a single atom behavior. Secondly, the magnetic moment is *rising* with temperature. This temperature dependence might be a fingerprint of Kondo screening of the moments on Mn atoms, though one can consider as an explanation the local environment effect as well.

Since the physical picture of large magnetic moments on Mn atoms diluted in a disordered Al matrix is most likely a

correct one, we may further study the detailed character of this magnetic state. It is well-known that the indirect [Ruderman-Kittel-Kasuga-Yosida (RKKY)] interaction between solute atoms in a disordered matrix could result in a spin-glass state, which is a manifestation of random magnetic order.¹⁸ As has been indicated by Pettifor,¹⁹ the reason why Mn and Fe are close to a *disordered local moments* regime is because they have a half-filled d shell and, correspondingly, a large Fermi momentum. The latter would lead to a short spatial period of the RKKY oscillations and, therefore, to frustration in the direction of moments if there is atomic disorder. The antiferromagnetic sign of the Mn-Mn interaction was suggested by Hauser *et al.*⁵ for the case of Al-Mn amorphous alloys and quasicrystals. However, in calculations using the Korringa-Kahn-Rostoker-KKR Green's-function method the Mn-Mn interaction in fcc Al appeared to be of a *ferromagnetic* sign.¹¹ It means that only topological disorder can produce the random sign of the RKKY interaction on different Mn sites and, therefore, frustrate the otherwise ferromagnetic order.

To gain more insight into the magnetic structure of Al-Mn liquids we have performed and report here local-spin-density approximation (LSDA) calculations for $\text{Al}_{100-x}\text{Mn}_x$ allowing for *arbitrary* directions of local magnetic moments. Noncollinear spin structures can be calculated within the LSDA,²⁰ but there are very few applications for disordered systems using the supercell linear muffin-tin orbital (LMTO) method²¹ or the "LMTO-derived" tight-binding Hubbard model with a fixed Stoner exchange integral.²² In the present work we have implemented and made use of the method,²⁰ within the *ab initio* real-space tight-binding LMTO formalism (RSTB), successfully applied before for studies of collinear magnetism in disordered Fe-B and Ni-B,²³⁻²⁵ and Al-Mn systems,¹⁶ and we now apply it to self-consistent calculations of the noncollinear magnetic $\text{Al}_{100-x}\text{Mn}_x$ liquids with $x=15, 20$, and 40 .

II. ELECTRONIC STRUCTURE CALCULATIONS WITH NONCOLLINEAR REAL-SPACE TIGHT-BINDING LMTO

In a system with noncollinear magnetic order the electrons experience an exchange field which depends on the local orientation of the magnetic moment at each atomic site R ,²⁶ and it can be written, in the local-density approximation, as²⁰

$$V_{\sigma\sigma'}^{xc}(\mathbf{r}) = -\frac{1}{2}\Delta_{xc}(n, m; \mathbf{r})\vec{e}_R \cdot \vec{\sigma}, \quad (1)$$

where $n \equiv n(\mathbf{r})$ and $m \equiv |\vec{m}(\mathbf{r})|$ are the local electron and spin densities, respectively, and $\vec{e}_R = [\cos(\phi_R)\sin(\theta_R), \sin(\phi_R)\sin(\theta_R), \cos(\theta_R)]$ is the direction of the moment on site R with respect to the global coordinate system, $\vec{\sigma}$ is the Pauli spin matrix in standard representation. All these quantities should be found self-consistently and this constitutes a complicated problem. We have treated it as follows.

In constructing the *ab initio* Hamiltonian H , we have made use of the method of Andersen and Jepsen²⁷ and transformed H into a tight-binding form to make use of the real-space recursion method. The overlap and Hamiltonian matrices

in the tight-binding LMTO method were expressed via a *two-center* Hamiltonian h^α , which for a noncollinear case takes the following form:

$$h^\alpha = c^\alpha - E_\nu + \sqrt{d^\alpha}(US^\alpha U^\dagger)\sqrt{d^\alpha}, \quad (2)$$

where $S^\alpha \equiv S_{R'L'RL}^\alpha$ is the spin-independent matrix of the localized structure constants, c^α and d^α are the matrices of potential parameters, diagonal in spin space, E_ν are the reference energies chosen at the centers of the respective bands, U is the standard spin- $\frac{1}{2}$ rotation matrix,

$$U = \begin{pmatrix} \exp(i\phi_R/2)\cos(\theta_R/2) & \exp(-i\phi_R/2)\sin(\theta_R/2) \\ -\exp(i\phi_R/2)\sin(\theta_R/2) & \exp(-i\phi_R/2)\cos(\theta_R/2) \end{pmatrix}, \quad (3)$$

and $U_{ij}^\dagger = U_{ji}^*$.

In practice, to make use of the recursion method, we have constructed a nearly orthonormal representation starting from the most localized tight-binding (TB) Hamiltonian h^α , Eq. (2), rotated such that we obtain the Hamiltonian matrix in the global coordinate system,

$$\begin{aligned} H^\gamma &= U^\dagger(E_\nu + h^\alpha(1 - o^\alpha h^\alpha)^{-1})U \\ &= U^\dagger(E_\nu + h^\alpha - h^\alpha o^\alpha h^\alpha + \dots)U. \end{aligned} \quad (4)$$

This orthonormalized Hamiltonian in the atomic-sphere approximation (ASA) has been used in the present work to *second order* in the $E - E_\nu$ expansion. The local density-of-states matrices $N_{R\sigma, R\sigma'}(E) = -1/\pi \text{Im}\langle R\sigma | (E - H + i0)^{-1} | R\sigma' \rangle$ have been found by the recursion method with the Hamiltonian H^γ , Eq. (4), and the band edges have been estimated according to Beer and Pettifor.²⁸ The orientation of a local-spin quantization axis can be easily found (in the ASA) by diagonalizing the density matrix integrated over the atomic spheres, $q_{\sigma\sigma'} = \int_{S_R} \rho_{\sigma\sigma'}(\mathbf{r}) d^3r$, yielding the angles,²⁰

$$\tan(\theta) = \frac{2|q_{12}|}{q_{11} - q_{22}}, \quad \tan(\phi) = -\text{Arg}(q_{12}). \quad (5)$$

It should be noted that the present is an $O(N)$ LDA scheme because we work in real space with the use of the recursion method. As usual, we expect it to become superior to k -space methods for large systems. Our rough estimate shows that the crossover point is at about 50–60 inequivalent atoms. Moreover, the present method is intrinsically parallelizable, and we have made use of this advantage.

III. RESULTS AND DISCUSSION

A. fcc Fe

In the first instance, we have applied the method to the well-known problem of fcc Fe in order to compare the results with those calculated by the ASW method.²⁹ The results are shown in Table I. They show a consistent agreement with each other for different atomic densities. Our data (Table I) illustrates two important points: (i) the effect of accuracy in the construction of the Hamiltonian and (ii) the convergence of calculated quantities.

TABLE I. The parameters of the noncollinear fcc Fe: the comparison of the real-space tight-binding LMTO (RSTB) and the ASW methods; 42 neighbors were used for constructing the Hamiltonian H^γ if not indicated otherwise; $\Delta_{\max} = \max|\cos\theta_{ij} - \langle\cos\theta_{ij}\rangle|$. In noncollinear ASW calculation $\cos\theta_{ij} = \langle\cos\theta_{ij}\rangle = -1/3$.

S (a.u.)	Moment on Fe (μ_B)		ΔE (Ry)		$\langle\cos\theta_{ij}\rangle$	Δ_{\max}
	RSTB	ASW	RSTB	ASW	RSTB	RSTB
2.82	2.72	2.69	0.085	0.093	Ferromagnetic	
2.79	2.66	2.65	0	0	Ferromagnetic	
2.79 ^a	2.50	2.65	-0.001	0	Ferromagnetic	
2.655 ^a	1.24 ^b	1.54	-0.037	-0.039	-0.3329	0.08
	1.27 ^c	1.54	-0.037	-0.039	-0.3332	0.03

^aWith the use of 18 nearest neighbors for H^γ .

^bAfter 150 iterations to achieve self-consistency.

^cAfter 300 iterations.

We have found that in order to calculate the magnetic moments and total energies at the same level of accuracy as achieved with the k -space method, it is important to construct the Hamiltonian very accurately, by including up to 42 neighboring atoms. If one takes 18 (first and second) neighbors only, the magnetic moment on Fe drops from the correct value of $2.66\mu_B$ down to $2.50\mu_B$ at the atomic-sphere radius $S = 2.79$ a.u. (Table I).

Concerning the convergence of the method, we have checked for $S = 2.655$ a.u. what the most stable magnetic structure is and we found it to be a noncollinear one. The total energy of this noncollinear structure relative to the ferromagnetic configuration at $S = 2.79$ a.u. approaches -37 mRy in the RSTB method compared to -39 mRy in the ASW. The magnetic moment comes out to be somewhat smaller than that in the ASW calculations (1.3 vs $1.54\mu_B$). The state with lowest energy has been, however, predicted correctly with the Fe moments pointing towards the center of the cubic cell, thus showing the reliability of the RSTB method.

B. Al-Mn liquid

For our RSTB-LMTO calculations of the electronic structure we have taken 60 atom structural models for liquid $\text{Al}_{60}\text{Mn}_{40}$ and $\text{Al}_{80}\text{Mn}_{20}$, and 56 and 98 atom models for liquid $\text{Al}_{84}\text{Mn}_{14}$. The structural models were constructed by means of a standard Monte Carlo method with bond-order potentials to account properly for the covalent interactions in Al-Mn systems (for details see Ref. 16). Comparing the radial distribution functions for these structures with ones for 666-atom clusters from Ref. 16, we have found that they are close to those calculated with smaller size models. The bond lengths and coordination numbers were found to be quite close in $\text{Al}_{86}\text{Mn}_{14}$ to those in $\text{Al}_{80}\text{Mn}_{20}$. The topological short-range order in $\text{Al}_{60}\text{Mn}_{40}$ is quite different from that in $\text{Al}_{80}\text{Mn}_{20}$: in the former we have $Z_{\text{MnMn}} = 3.38$ for the Mn-Mn coordination number, whereas in the latter Z_{MnMn} is just 1.36. There are no Mn-Mn pairs in $c\text{-Al}_6\text{Mn}$, and their coordination number is very small in the $\text{Al}_{86}\text{Mn}_{14}$ liquid. The analysis of bond angles shows some tendency for $\text{Al}_{86}\text{Mn}_{14}$ and $\text{Al}_{80}\text{Mn}_{20}$ liquids to have an icosahedral motif.¹⁶

We have performed calculations, assuming both collinear and noncollinear arrangements of spins, for $\text{Al}_{100-x}\text{Mn}_x$ liquids of different compositions. We have found a strong tendency for magnetic moments on Mn to have large absolute values and orientational disorder (in the noncollinear case), so that the net magnetic moment averages to a very low value, which is almost zero for $\text{Al}_{84}\text{Mn}_{14}$. It is important to note that for $c\text{-Al}_6\text{Mn}$ our noncollinear calculations yielded a nonmagnetic state, in accordance with our previous discussion of the role of the van Hove singularity at the Fermi level in the density of states of this system.¹⁶

To construct the continued fractions needed for the recursions we have used up to ~ 1200 -atom clusters built from our “supercells” by applying periodic boundary conditions. For these systems we have used nine recursion levels for the s and p electrons and 18 levels for the d electrons of the Mn atoms, and eight recursion levels for the Al electrons.

We have found that all average values in the present calculations are close to our previous results¹⁶ based on large structural models and averaged self-consistent potential parameters (Fig. 1, Table II, III). Moreover, it is worth noting that in the collinear case we have found no meaningful changes in the distribution of the local magnetic moments, in marked distinction from what has been obtained in Ref. 22 for amorphous Fe, although in Ref. 16 the values of Mn magnetic moment are somewhat larger. For $\text{Al}_{84}\text{Mn}_{14}$ system the averages are in good agreement for small ($N=56$) and large ($N=98$) calculated cells in spite of rather small statistics for Mn in the former calculation.

The analysis of the densities of states projected onto the local magnetization axes reveals that the total electronic density of states (DOS) has a sharp peak for majority spins in all liquid Al-Mn alloys at about -2.5 eV below the Fermi level (Fig. 2), and a peak in the unoccupied minority spin band at about $+1$ eV. The local projected DOS's are similar to those calculated in our previous work.¹⁶ The difference between collinear and noncollinear DOS grows with increasing Mn concentration (Figs. 1, 2). We note that the shape of the majority/minority DOS reflects a non-rigid-band behavior (Fig. 1) which shows up in an asymmetric splitting of the Mn d band with respect to the Fermi level. This means that the rigid-band Stoner model is hardly applicable to this system.

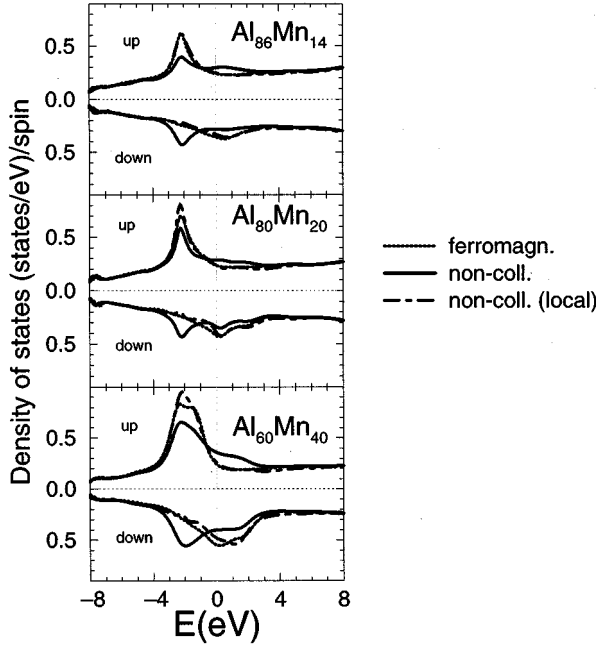


FIG. 1. The spin-polarized electronic density of states for Al-Mn liquids: (a) $\text{Al}_{84}\text{Mn}_{14}$, (b) $\text{Al}_{80}\text{Mn}_{20}$, and (c) $\text{Al}_{60}\text{Mn}_{40}$. Solid line: density of states for a global quantization axis, noncollinear configuration; dot-dashed line: the same for a local quantization axis; dotted line: the density of states per spin for the collinear case.

We have found that the noncollinear state is more stable compared to the collinear one, being lower in energy by about 0.025 Ry (Table II). The average value of the Mn moment in our calculation is almost independent of the manganese concentration in correspondence with the experiment described in Ref. 17.

In our calculations the distribution of the absolute values of the Mn moment is asymmetric in $\text{Al}_{86}\text{Mn}_{14}$ and $\text{Al}_{80}\text{Mn}_{20}$, and it is biased towards higher values, whereas the moment distribution in $\text{Al}_{60}\text{Mn}_{40}$ is symmetric (Fig. 3). To gain more insight into the spatial distribution of the moments on Mn we have analyzed the average cosine of an angle between the moments, $\langle \cos(\theta_{ij}) \rangle$. We have found that $\langle \cos(\theta_{ij}) \rangle$ is positive and rather large for neighboring atoms separated by $R_{ij} < 4.7 \text{ \AA}$ (Table III) and negative for next neighbors, $4.7 \text{ \AA} < R_{ij} < 6.1 \text{ \AA}$ [for the Mn impurity in fcc-Al

TABLE II. The results for collinear spin configurations. $\mu_{\min} - \mu_{\max}$ is the interval spanned by the values of Mn moments; $\langle \mu_{\text{Mn}} \rangle$ and $\langle \mu_{\text{Al}} \rangle$ are the average values of the moment on Mn and Al, respectively. μ is the value of the average moment per atom. Data in parentheses are for the models with $N=56$ atoms. Directions of Al moments are opposite to Mn moments.

	$\text{Al}_{60}\text{Mn}_{40}$	$\text{Al}_{80}\text{Mn}_{20}$	$\text{Al}_{86}\text{Mn}_{14}$
$\mu_{\min} - \mu_{\max}$	1.96–3.08	1.28–3.39	1.62–3.49
$\langle \mu_{\text{Mn}} \rangle$	2.68	2.72	2.84 (2.87)
$\langle \mu_{\text{Al}} \rangle$	0.096	0.048	0.039 (0.040)
μ	1.01	0.51	0.37 (0.38)
μ_{Mn}^a	2.87	3.17	3.29

^aThe result of collinear calculation (Ref. 16).

TABLE III. The results for noncollinear spin configurations. $\mu_{\min} - \mu_{\max}$ is the interval spanned by the values of Mn moments; $\langle \mu_{\text{Mn}} \rangle$ and $\langle \mu_{\text{Al}} \rangle$ are the average of the moment value on Mn and Al, respectively. μ is the value of the average moment per atom; $\langle \vec{e}_i \vec{e}_j \rangle_{\text{Mn}}$ is the average cosine of angle between moments on two neighboring Mn atoms ($|\vec{e}_i| = 1$). $E_{\text{fm}} - E_{\text{nc}}$ is the energy difference between ferromagnetic and noncollinear configurations. All the moments are in units of μ_B , data for $N=56$ atoms are in parentheses.

	$\text{Al}_{60}\text{Mn}_{40}$	$\text{Al}_{80}\text{Mn}_{20}$	$\text{Al}_{86}\text{Mn}_{14}$
$\mu_{\min} - \mu_{\max}$	2.05–3.43	1.42–3.54	1.86–3.39
$\langle \mu_{\text{Mn}} \rangle$	2.74	2.89	2.88(2.91)
$\langle \mu_{\text{Al}} \rangle$	0.062	0.036	0.029(0.030)
μ	0.27	0.23	0.08(0.03)
$E_{\text{fm}} - E_{\text{nc}}$ (Ry)	0.025	0.024	0.026(0.026)
$\langle \vec{e}_i \vec{e}_j \rangle_{\text{Mn}}$			
$R_{ij} < 4.7 \text{ \AA}$	0.22	0.42	0.13
$4.7 \text{ \AA} < R_{ij} < 6.1 \text{ \AA}$	-0.09	-0.21	-0.25

it corresponds to first- and second-nearest neighbors in the former case and third neighbors in the latter (inset in Fig. 4)]. It is instructive to analyze the average cosine of the angle between Mn moments, $\cos(\theta_{ij})$, as a function of the distance R_{ij} between them (Fig. 4), in conjunction with the Mn-Mn partial radial distribution function. For $\text{Al}_{86}\text{Mn}_{14}$ liquid the nearest neighbors are likely to be subject to a ferromagnetic interaction, whereas other studied systems display a definite antiferromagnetic sign of the interaction between nearest Mn atoms which changes quickly into ferromagnetic with increasing separation. It makes these systems quite different compared to Mn in fcc Al where the exchange has a ferro-

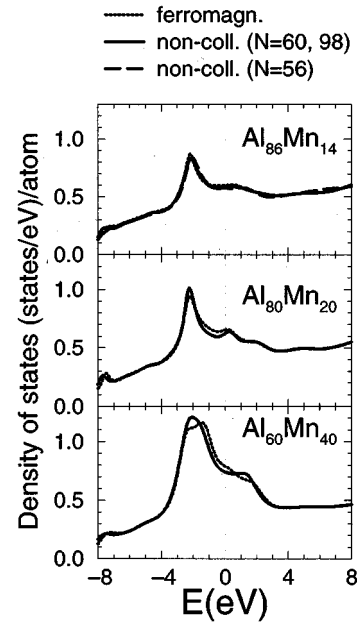


FIG. 2. The total electronic density of states per atom for Al-Mn liquids: (a) $\text{Al}_{84}\text{Mn}_{14}$, (b) $\text{Al}_{80}\text{Mn}_{20}$, and (c) $\text{Al}_{60}\text{Mn}_{40}$. The solid and dotted lines are results of noncollinear and collinear calculations, the dashed line is for a smaller structural model of liquid $\text{Al}_{84}\text{Mn}_{14}$.

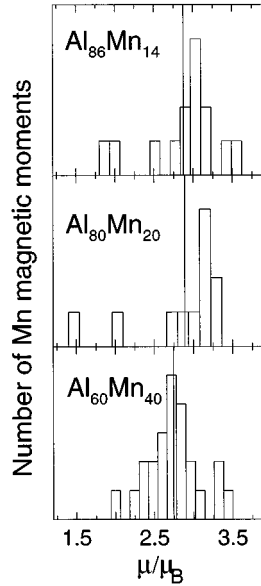


FIG. 3. The histogram of the moment distribution in Al-Mn liquids. The vertical line marks the center of gravity of the distribution. Note the pronounced asymmetry in the distribution in the case of $\text{Al}_{84}\text{Mn}_{14}$ and $\text{Al}_{80}\text{Mn}_{20}$ compared to the symmetric distribution in $\text{Al}_{60}\text{Mn}_{40}$.

magnetic sign up to third neighbors:¹¹ topological disorder produces RKKY exchange constants of random signs and the resulting frustration causes the random directional order of moments on the manganese atoms. For distant neighbors we have found a preference for an antiferromagnetic alignment of the Mn moments.

IV. CONCLUSIONS

The present results confirm our earlier prediction that topological disorder is the main driving force for the formation of a large ($\mu_{\text{eff}} \sim 2.8\mu_B$) magnetic moment on Mn in Al-Mn liquids.¹⁶ This value is close to the single-impurity limit,³ and is not sensitive to interaction with other Mn atoms in the alloy, as recently found experimentally.¹⁷

It is a popular view that, at low temperatures, only a fraction of the Mn sites in disordered Al-Mn/Al-Mn-Pd systems carry a moment due to a strong local environment effect with the remainder being nonmagnetic.^{8,30,31,17} A similar view has been applied in Ref. 17 to make an interpretation of their measurements in the molten state at high temperatures. These authors concluded that about 60% of the Mn atoms can be nonmagnetic only if the rest of them carry moments of more than $5\mu_B$. Our results, however, do not confirm this view.

We have found that *all* Mn sites are magnetic in the systems we studied (Table III) though the absolute values scatter a lot (from 1.42 to $3.54\mu_B$ in $\text{Al}_{80}\text{Mn}_{20}$, for instance). As we have mentioned above, at low temperatures Mn atoms can be in a Kondo-compensated spin state which disappears with increasing temperature. The observed rise in magnetic susceptibility χ above the melting point in Al-Pd-Mn systems¹⁷

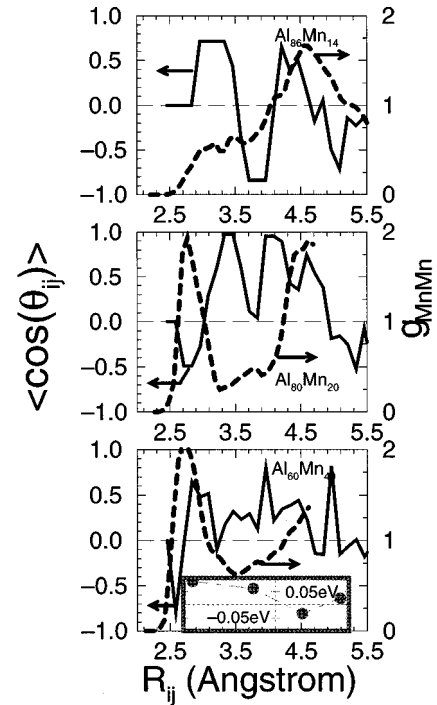


FIG. 4. The cosine of the angle between two Mn moments (solid line) and partial Mn-Mn radial distribution functions (dashed line, right axis). These results demonstrate a fine balance between the ferromagnetic and antiferromagnetic signs of interaction and its rapid variation with distance, as can be reliably guessed from the resulting angle distribution between the Mn moments shown in this figure. Inset: the data of T. Hoshino (Ref. 11) for the energy difference between the antiferromagnetic and ferromagnetic Mn dimer in fcc Al. Calculations have been performed for the distance between Mn atoms in the dimer corresponding to first-, second-, third-, and fourth-nearest-neighbor separations in fcc-Al matrix.

is quite the opposite to what is expected from the usual spin-fluctuation theories where χ is Curie-like and, therefore, decreases with temperature.³² It could be a fingerprint of Kondo unscreening with increasing temperature, but it could also be a result of a variation of the moments distribution (Fig. 3) with temperature and local environment effects, facts which should be analyzed further. We predict that Al-Mn liquids have a random magnetic order with predominance of ferromagnetic interactions for nearest Mn neighbors, and noncollinearity is triggered by random RKKY interaction between solute atoms of Mn in a disordered Al matrix.

ACKNOWLEDGMENTS

The authors are indebted to V. Heine, J. Kübler, D. Nguyen Manh, A. Pasturel, D. Pettifor, L. Sandratskii, and M. Uhl for helpful discussions. A.V.S. has been supported by the Alexander von Humboldt Foundation. We acknowledge the provision of computer facilities, used for the part of this work, by the Materials Modelling Laboratory at Oxford University. The calculations have been performed on the vector-parallel computer Fujitsu/SNI VPP500/4 at the Computer Center of TH Darmstadt.

- *Permanent address: Kurchatov Institute, 123182 Moscow, Russia.
- [†]Author to whom correspondence should be addressed.
- ¹For a review, see J. Friedel, in *Metallic Solid Solutions* (Benjamin, New York, 1963), p. 1.
- ²P. W. Anderson, *Phys. Rev. B* **124**, 41 (1961).
- ³J. R. Cooper and M. Miljak, *J. Phys. F* **6**, 2151 (1976).
- ⁴D. Schechtman, I. Blech, D. Gratias, and J. W. Cahn, *Phys. Rev. Lett.* **53**, 1951 (1984).
- ⁵J. J. Hauser, H. S. Chen, and J. V. Waszczak, *Phys. Rev. B* **33**, 3577 (1986); J. J. Hauser, H. S. Chen, G. P. Espinosa, and J. V. Waszczak, *ibid.* **34**, 4674 (1986).
- ⁶M. Maret, A. Pasturel, C. Senillou, J. M. Dubois, and P. Chieux, *J. Phys. (Paris)* **5**, 295 (1989); M. Maret, P. Chieux, J. M. Dubois, and A. Pasturel, *J. Phys. Condens. Matter* **3**, 2801 (1991).
- ⁷T. Goto, T. Sakakibara, and K. Fukamichi, *J. Phys. Soc. Jpn.* **57**, 1751 (1988).
- ⁸C. Berger and J. J. Préjean, *Phys. Rev. Lett.* **64**, 1769 (1990).
- ⁹R. M. Nieminen and M. Puska, *J. Phys. F* **10**, L123 (1980).
- ¹⁰J. Deutz, P. H. Dederichs, and R. Zeller, *J. Phys. F* **11**, 1787 (1981).
- ¹¹T. Hoshino, R. Zeller, P. H. Dederichs, and M. Weinert, *Europhys. Lett.* **24**, 495 (1993); T. Hoshino (private communication).
- ¹²D. Bagayoko, N. Brener, D. Kanhere, and J. Callaway, *Phys. Rev. B* **36**, 9263 (1987); Yang Jinlong, Lan Huibin, Wang Kelin, L. F. Donà dalle Rosa, and F. Toigo, *ibid.* **44**, 10 508 (1991).
- ¹³M. E. Henry, D. D. Vvedensky, M. E. Eberhart, and R. C. O'Handley, *Phys. Rev. B* **37**, 10887 (1988).
- ¹⁴Feng Liu, S. N. Khanna, L. Magand, P. Jena, V. de Conlon, F. Reuse, S. S. Jaswal, X.-G. He, and F. Cyrot-Lackman, *Phys. Rev. B* **48**, 1295 (1993).
- ¹⁵M. Godinho, C. Berger, J. C. Lasjaunias, K. Hasselbach, and O. Bethoux, *J. Non-Cryst. Solids* **117-118**, 808 (1990).
- ¹⁶A. M. Bratkovsky, A. V. Smirnov, D. Nguyen-Manh, and A. Pasturel, *Phys. Rev. B* **52**, 3056 (1995).
- ¹⁷F. Hippert, M. Audier, H. Klein, R. Bellissent, and D. Boursier, *Phys. Rev. Lett.* **76**, 54 (1996).
- ¹⁸J. M. D. Coey, *Can. J. Phys.* **65**, 1210 (1987).
- ¹⁹D. G. Pettifor, *J. Magn. Magn. Mater.* **15-18**, 847 (1980).
- ²⁰J. Sticht, K.-H. Höck, and J. Kübler, *J. Phys. Condens. Matter* **1**, 8155 (1989).
- ²¹M. Liebs, K. Hummler, and M. Fähnle, *Phys. Rev. B* **51**, 8664 (1995).
- ²²R. Lorenz and J. Hafner, *J. Magn. Magn. Mater.* **139**, 209 (1995).
- ²³A. M. Bratkovsky and A. V. Smirnov, *Phys. Rev. B* **48**, 9606 (1993).
- ²⁴A. M. Bratkovsky and A. V. Smirnov, *J. Phys. Condens. Matter* **5**, 3203 (1993).
- ²⁵A. M. Bratkovsky, S.N. Rashkeev, A. V. Smirnov, and G. Wendin, *Europhys. Lett.* **26**, 43 (1994).
- ²⁶M. V. You and V. Heine, *J. Phys. F* **12**, 177 (1982).
- ²⁷O. K. Andersen and O. Jepsen, *Phys. Rev. Lett.* **53**, 2571 (1984).
- ²⁸N. Beer and D. Pettifor, in *The Electronic Structure of Complex Systems*, edited by P. Phariseau and W. M. Temmerman (Plenum, New York, 1984) p. 769.
- ²⁹M. Uhl, L. M. Sandratskii, and J. Kübler, *J. Magn. Magn. Mater.* **103**, 314 (1992); M. Uhl (private communication).
- ³⁰M. A. Chernikov, A. Bernasconi, C. Beeli, A. Schilling, and H. R. Ott, *Phys. Rev. B* **48**, 3058 (1993).
- ³¹J. C. Lasjaunias, A. Sulpice, N. Keller, and J. J. Préjean, *Phys. Rev. B* **52**, 886 (1995).
- ³²T. Moriya, *J. Magn. Magn. Mater.* **14**, 1 (1979).